COMPARISON OF THE PRANDTL MODEL WITH K(z) AND NON ZERO f WITH DOPPLER SODAR OBSERVATIONS

Iva Kavčič[1], Branko Grisogono[1], Ian A. Renfrew[2], Philip S. Anderson[3], Željko Večenaj[1], Ivana Stiperski[4]

[1]Department of Geophysics, Faculty of Science, University of Zagreb, Croatia
[2]School of Environmental Sciences, University of East Anglia, UK
[3]British Antarctic Survey, Cambridge, UK
[4]Hydrological and Meteorological Service, Croatia
E-mail: *ivakavc@gfz.hr*

Abstract: We present the analytical and numerical solutions for *(U, V)* depending on *(z, t)* in the katabatic flow, where *U* and *V* are the downslope and cross-slope wind components. The solutions for (*U, V*) from the recently extended analytical 1D Prandtl model are verified against observations (the 15-min averages) from a novel autonomous Doppler sodar wind profiling system in Antarctica. Two cases of the wintertime, primarily katabatically driven, flows with the different stability values are investigated. The analytical and numerical model parameters are calculated from the Doppler sodar and AWS (automatic weather station) data. Observations of the downslope component are generally better described by the model solutions, especially in the case of the stronger stability. The model solutions for *V* agree qualitatively with the observations, but are not accurate enough in determining the height and the speed of the *V* maximum. Therefore, further improvements of the Prandtl model will be amendable as well as recommendations for a better parameterization of katabatic flows in large-scale numerical models.

1. INTRODUCTION

Katabatic flows are regular features of stable atmospheric boundary layers (ABL) over inclined radiatively cooled surfaces, especially over glaciers. They play an important part in the atmospheric general circulation at high latitudes (e.g. Parish and Bromwich, 1991; Renfrew 2004) and thus have significant impact on the climate of areas such as Antarctica and Greenland (e.g. Parmhed et al., 2004; Renfrew and Anderson, 2006). The pure katabatic flow and its turbulence are characterized by a pronounced shallow low-level jet (LLJ) and sharp near-surface vertical temperature gradient (e.g. Grisogono and Oerlemans, 2001; Van den Broeke et al., 2002). Renfrew (2004) and Renfrew and Anderson (2006) show that significant katabatic flows over Antarctica most often exhibit clearly their LLJ and an anticlockwise backing of the wind with height.

Even a fine-scale nonhydrostatic numerical weather prediction (NWP) models encounters problems in modelling katabatic flows. In order to capture the jet-shaped shallow flow, which largely dominates the ABL turbulence, a model set-up with high vertical resolution is required (e.g. Renfrew, 2004). Therefore, these widespread flows typically have to be parameterized in large- and meso-scale models (e.g. Zilitinkevich et al., 2006). A simple Prandtl model of katabatic flows represents a balance between the negative buoyancy production due to the surface potential temperature deficit and dissipation by turbulent fluxes (e.g. Mahrt, 1982; Egger, 1990). Stiperski et al. (2007) extended the Prandtl model by including the Coriolis force in order to be able to cover long polar slopes and the corresponding long-lived strongly stable ABL. Kavčič and Grisogono (2007) introduced gradually varying eddy diffusivity in the analytical model of Stiperski et al. (2007).

Here we compare the analytical solutions for katabatic flows from Kavčič and Grisogono (2007) with the observations (the 15-min averages) from a novel autonomous Doppler sodar wind profiling system (for the detailed system description see Anderson et al., 2005). Both the analytical model assumptions and the related soundings over the wintertime Antarctica correspond to "primarily katabatic driven" flows where the influence from larger-scale weather systems is reduced (Renfrew, 2004; Renfrew and Anderson, 2002). The emphasis here is put on the height and speed of the low-level jet.

2. ANALYTICAL SOLUTIONS AND DATA

2.1 The extended Prandtl model

The rotating Prandtl model describes a hydrostatic, linear, one-dimensional Boussinesq flow with the effects of the Coriolis force included (Stiperski et al., 2007). As in the classical Prandtl model (e.g. Mahrt, 1982; Egger, 1990; Parmhed et al., 2004), the K-theory is invoked to model the turbulent fluxes. Kavčič and Grisogono (2007) obtained solutions of the rotating model for the case of non-constant K by using the WKB method (after Wentzel, Kramers and Brillouin, who popularized the method in theoretical physics) of zero-order (e.g. Bender and Orszag, 1978). We briefly list the WKB solutions for the the downslope and cross-slope components of the wind vector (U, V):

$$U_{WKB}(z) = \frac{C\sigma_0^2}{\gamma \sin(\alpha)} \exp\left(-\frac{\sigma_{WKB}(z)}{\sqrt{2}}\right) \sin\left(\frac{\sigma_{WKB}(z)}{\sqrt{2}}\right), \tag{1}$$

$$V_{WKB}(z,t) = \frac{Cf \cot(\alpha)}{\Pr \gamma} \left[1 - erf\left(\frac{I(z)}{2\sqrt{t}\Pr}\right) - \exp\left(-\frac{\sigma_{WKB}(z)}{\sqrt{2}}\right) \cos\left(\frac{\sigma_{WKB}(z)}{\sqrt{2}}\right)\right], \tag{2}$$

$$\sigma_{WKB}(z) = \sigma_0 I(z), \; \sigma_0^4 = \frac{N^2 \Pr \sin^2(\alpha) + f^2 \cos^2(\alpha)}{\Pr^2}, \; I(z) = \int_0^z K(z)^{-1/2} dz, \tag{3}$$

where the prescribed K-profile is (see Grisogono and Orlemans (2001))

$$K(z) = K_{\max} \sqrt{e} \frac{z}{h} \exp\left(-\frac{z^2}{2h^2}\right), K_{\max} = 3K_c, \tag{4}$$

with $K(z)$ reaching its maximum at the suitable height $h = 200$ m. Here the z axis is perpendicular to the surface (x axis) sloped with the negative (clockwise) angle α from the horizontal. The symbols have their usual meaning: K_c is a constant eddy diffusivity, θ_0 is a reference potential temperature, f is the Coriolis parameter, g is acceleration due to gravity, Pr is the turbulent Prandtl number, $N^2 = g\gamma/\theta_0$ is the buoyancy (Brunt-Vaisala) frequency and $C < 0$ is the constant surface-potential-temperature deficit (total minus the background potential temperature), applied to an undisturbed atmosphere-surface interface. Slope angle α, for which the katabatic wind is successfully treated by the model, typically does not exceed $\sim 10°$, therefore giving a reasonable assumption of using the constant gradient of the background potential temperature γ in the true vertical. The WKB solutions (1) and (2) hold after a typical period $T = 2\pi/(N\sin(\alpha))$ (Mahrt, 1982; Grisogono, 2003); note that V diffuses upward in time, t. For further details about the total flow vector (U, V, θ) (θ is the potential temperature perturbation, not discussed here) see Kavčič and Grisogono (2007) or Stiperski et al. (2007).

2.2 Doppler sodar and AWS data

We compare the analytical wind profiles with the data gathered during the extensive year-round observations of the vertical structure of katabatic flow over Coats Land, Antarctica from 2002 and 2003 (Renfrew and Anderson, 2006). The wind profiles (15-min averages) are derived from an autonomous Doppler sodar sounding system installed on a moderate slope (around 5% at most) some 50 km south of Halley Research Station (Anderson et al., 2005). Two sodar settings were used: high vertical resolution with frequency = 502 Hz, range gates $\sim$ 10-70 m, height $\sim$ 20-500 m, and standard vertical resolution with frequency = 506 Hz, range gates $\sim$ 20-60m, height $\sim$ 20-500 m.

The values of C and γ for the WKB solutions are determined on the basis of real-time meteorological information provided by the *in situ* AWS data (at Halley and C1 to C4 sites, see Renfrew and Anderson (2006)) and the upper-air radiosonde soundings at Halley (Renfrew and Anderson, 2006). A subset of 16 wintertime days (and 805 profiles) was chosen according to the criteria for primarily katabatically driven flows, as described in Renfrew and Anderson (2002).

3. DISCUSSION AND CONCLUSIONS

The WKB solutions (1) and (2) are compared with the data from the C2 site (Renfrew and Anderson, 2006). Figures 1 and 2 show two of the total 16 cases investigated, selected as the "limit values" of the stability of free atmosphere described by γ. Values of γ are determined from the free atmosphere observations at Halley, see Table 3 in Renfrew and Anderson (2006). In the first case, August 28th 2003 (12 h – 21 h), $\gamma = 0.016$ Km[-1] and C = -9.3°C. For the second case, 8th September 2003 (10 h – 15 h), $\gamma = 0.001$ Km[-1] and C = -4.6°C. The surface potential-temperature-deficit C is calculated as the total θ (approximated with the AWS data for θ at 1 m) minus the background θ determined from the upper-air soundings at Halley. The slope α at C2 site is -3.14°, and f is negative (Renfrew and Anderson, 2006). The numerical model top is set at 2000 m, and $Pr = 1.1$.

In both Fig. 1 and 2 the WKB solutions (solid) agree well with the corresponding time-dependent numerical solutions (dashed) for U and V (Kavčič and Grisogono, 2007). The agreement is better for the stronger stability (Fig. 1). Also, for the stronger stability the sodar data (blue asterisks) for U are better described with (1), especially in capturing the height (Fig. 1) of LLJ maximum. The strength of LLJ maximum is underestimated on average (Fig. 1a) but well described for the particular time (Fig. 1b, 12:46). However, V_{WKB} largely underestimates the magnitude of the cross-slope component (Fig.1, red asterisks), although it qualitatively describes its shape. The underestimation of an order of magnitude of V_{WKB} with the respect to the sodar data suggests that other effects, beyond the scope of improved Prandtl model, are here in play (e.g. 3D mesoscale effects). Decreased stability (the 2nd case, 8-Sep 2003, Fig. 2) seems to have the greater influence on the height of the maximum in the WKB and numerical solutions for V than for U. Moreover, the WKB solutions (1) and (2) generally overestimate both of the measured components (Fig. 2a, blue and red asterisks, respectively) in the second case. The height of LLJ maximum in U is still captured with a reasonable accuracy (Fig. 2). But, in this case the measured V maximum is closer to the measured maximum in U, yielding to an overestimation of the V maximum height by the V_{WKB} from (2). This study shows that the WKB solutions (1) and (2) may be applied to describe the observation data with some success. The agreement is generally better for the U than for the V component, raising the need for the further investigation of the cross-slope component dynamics. We hope that with the further development of the analytical Prandtl model and modifications of the varying eddy diffusivity profile, the WKB solutions will give a more realistic description of sloped flows, towards better surface-flux parameterizations in climate models and data analysis.

REFERENCES

Anderson, P. S., R. S. Ladkin, I. A. Renfrew, 2005: An autonomous Doppler sodar wind profiling system. *J. Atmos. And Ocean. Tech.* **22**: 1309-1325.

Bender, C. M., S. A. Orszag, 1978: *Advanced mathematical methods for scientists and engineers.* Mc Graw-Hill Inc. 593 pp.

Egger, J., 1990: Thermally forced flows: Theory, in W. Blumen (ed.), *Atmospheric processes over complex terrain.* AMS. 43-57.

Grisogono, B., 2003: Post-onset behaviour of the pure katabatic flow. *Boundary-Layer Meteorol.* **107**, 157-175.

Grisogono, B., J. Oerlemans, 2001: Katabatic flow: analytic solution for gradually varying eddy diffusivities. *J. Atmos. Sci.* **58**, 3349-3354.

Kavčič, I., B. Grisogono, 2007: Katabatic flow with Coriolis effect and gradually varying eddy diffusivity. Boundary-Layer Meteorol. Accepted.

Mahrt, L., 1982: Momentum balance of gravity flows. *J. Atmos. Sci.* **39**, 2701-2711.

Parish, T. R., D. H. Bromwich, 1991: Continental-scale simulation of the Antarctic katabatic wind regime. *J. Climate* **4**, 135-146.

Parmhed, O., J. Oerlemans, B. Grisogono, 2004: Describing the surface fluxes in the katabatic flow on Breidamerkurjokull, Iceland. *Quart. J. Roy. Meteorol. Soc.* **130**, 1137-1151.

Renfrew, I. A., 2004: The dynamics of idealized katabatic flow over a moderate slope and ice shelf. *Quart. J. Roy. Meteorol. Soc.* **130**, 1023-1045.

Renfrew, I. A., P. S. Anderson, 2002: The surface climatology of an ordinary katabatic wind regime in Coats Land, Antarctica. Tellus **54A**, 463-484.

Renfrew, I. A., P. S. Anderson, 2006: Profiles of katabatic flow in summer and winter over Coats Land, Antarctica. *Quart. J. Roy. Meteorol. Soc*. **132**, 779-882.

Stiperski, I., I. Kavčič, B. Grisogono, D. R. Durran, 2007: Including Coriolis effects in the Prandtl model for katabatic flow. *Quart. J. Roy. Meteorol. Soc.* **133**, 101-106.

Van den Broeke, M. R., N. P. M. van Lipzig, E. van Meijgaard, 2002: Momentum budget of the East-Antarctic atmospheric boundary layer: results of a regional climate model. *J. Atmos. Sci.* **59**, 3117-3129.

Zilitinkevich, S., H. Savijärvi, A. Baklanov, B. Grisogono, K. Myrberg, 2006: Forthcoming meetings on planetary boundary-layer theory, modelling and applications. *Boundary-Layer Meteorol.* 119, 591–593.
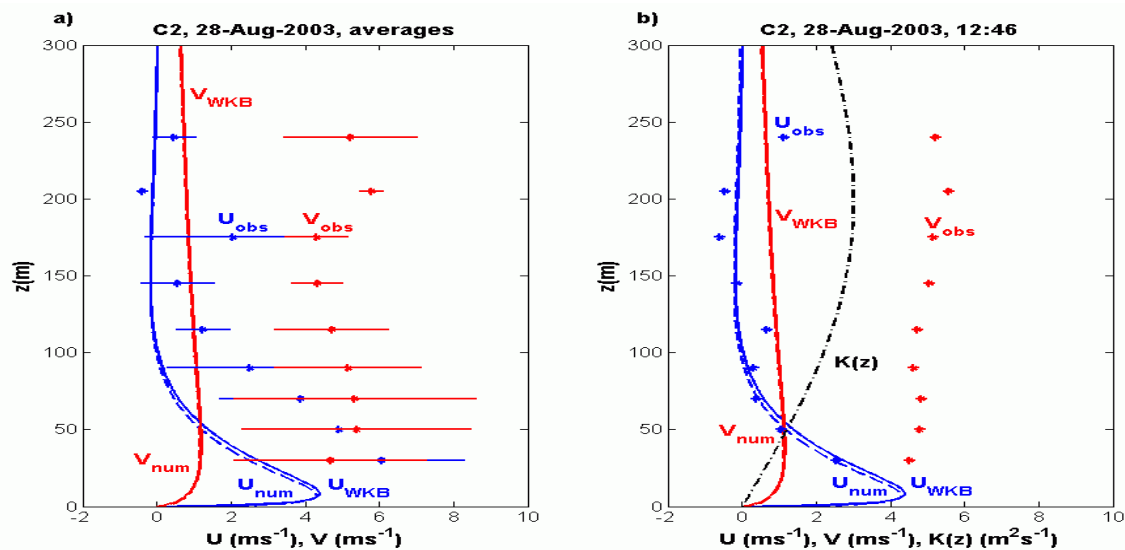
Figure 1: Comparison of numerical (dashed) and analytical WKB (solid) solutions for *U* (blue) and *V* (red), with the Doppler sodar data (blue and red asterisks with errorbars, respectively) for a) case averages and b) t=13:30 h (local time, about 1 h 40 min behind UTC). The WKB solutions hold after $T \approx 1.3$ h. Here $K(z)$ is from (4) with $K_{max} = 3$ m^2 s^{-1} at $h = 200$ m (black, dot-dashed); other parameters are $(f, \alpha, \gamma, Pr, C)$ = (-1.4×10^{-4} s^{-1}, −3.14°, 16×10^{-3} K m^{-1}, 1.1, −9.3°C).
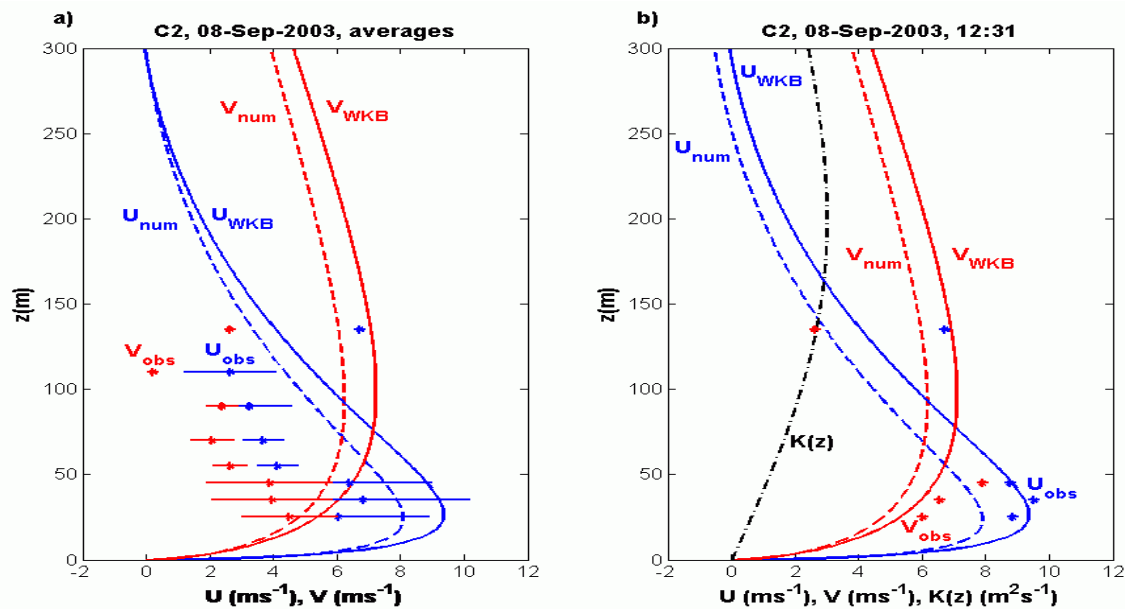

Figure 2: Comparison of numerical (dashed) and analytical WKB (solid) solutions for *U* (blue) and *V* (red), both of them valid after $T = 2\pi/(N \sin(\alpha)) \approx 5.2$ h, with the Doppler sodar data (blue and red asterisks with errorbars, respectively) for a) case averages and b) t=12:31 h (local time, about 1 h 40 min behind UTC). The WKB solutions hold after $T \approx 5.2$ h. Model parameters are $(f, \alpha, \gamma, Pr, C)$ = (-1.4×10^{-4} s^{-1}, −3.14°, 1×10^{-3} K m^{-1}, 1.1, −4.6°C). The rest as in Figure 1.